Neutrinos from active black holes, sources of ultra high energy cosmic rays

Julia K. Becker [a,b,*] and Peter L. Biermann [c,d,e,f,g]

[a] *Göteborgs Universitet, Institutionen för Fysik, SE-41296 Göteborg, Sweden*

[b] *Technische Universität Dortmund, Inst. f. Physik, D-44221 Dortmund, Germany*

[c] *Max Planck Institut f. Radioastr., Auf dem Hügel 69, D-53121 Bonn, Germany*

[d] *Dept. of Physics and Astronomy, University of Bonn, Germany*

[e] *Dept. of Physics and Astronomy, University of Alabama, Tuscaloosa, AL, USA*

[f] *Dept. of Physics and Astronomy, University of Alabama, Huntsville, AL, USA*

[g] *Inst. Nucl. Phys. FZ, Karlsruhe Inst. of Techn. (KIT), Karlsruhe, Germany*

Abstract

A correlation between the highest energy Cosmic Rays (above ~ 60 EeV) and the distribution of active galactic nuclei (AGN) gives rise to a prediction of neutrino production in the same sources. In this paper, we present a detailed AGN model, predicting neutrino production near the foot of the jet, where the photon fields from the disk and synchrotron radiation from the jet itself create high optical depths for proton-photon interactions. The protons escape from later shocks where the emission region is optically thin for proton-photon interactions. Consequently, Cosmic Rays are predicted to come from FR-I galaxies, independent of the orientation of the source. Neutrinos, on the other hand, are only observable from sources directing their jet towards Earth, i.e. flat spectrum radio sources and in particular BL Lac type objects, due to the strongly boosted neutrino emission.

Key words: UHECRs, radio galaxies, neutrinos, jet structure
PACS: 98.70.Sa, 98.54.Gr, 14.60.Lm

∗ Corresponding author. Contact: julia.becker@physics.gu.se, phone: +46-31-7723190

arXiv:0805.1498v3 [astro-ph] 18 Dec 2008

1 The underlying AGN model

The evidence for a correlation between the arrival directions of ultra high energy Cosmic Rays (UHECRs) with active galactic nuclei, as reported by the Auger Collaboration (2007, 2008), supports many long standing expectations (Ginzburg & Syrovatskii, 1964). The active galactic nuclei with the most detailed available theory to actually accelerate protons to beyond 10^{20} eV are radio galaxies (Biermann & Strittmatter, 1987). In all radio galaxies the feeding of outer radio emitting regions is done via a relativistic jet emanating from near a black hole. Shock waves in such jets can accelerate particles just as shocks in the Solar wind do [1]. Shocks in the jet emanating from near the black hole start around a few thousand gravitational radii, as it was shown with detailed spectral fits of the entire electromagnetic spectrum, including the spatial structure at the wavelengths where it is known. The shocks end as strong shocks at kpc or further out (Markoff et al., 2001, 2005). It was also shown that when particles get accelerated at the first shock, proton-photon interactions limit their maximal energy (Krülls, 1992; Nellen et al., 1993; Mannheim, 1995).

The correlation with the distribution of active galactic nuclei claimed by the Auger collaboration has been disputed by the HiRes collaboration (Abbasi et al., 2008a). However, it is not clear at this point, whether both data sets use the same lower energy cutoff with the same sharpness. This is important, as the MHD simulations of cosmic magnetic fields (Ryu et al., 2008; Das et al., 2008) show that scattering of ultra high energy particles rapidly increases with lower energy even near 60 EeV. Thus, with even a slight mismatch between the two data sets the statistics could be very skewed. Using a complete sample of radio galaxy sources and their predicted properties as UHECR sources, these statistics will be explored elsewhere (Caramete et al., 2008; Curuţiu et al., 2008; Duţan et al., 2008).

1.1 FR-I galaxies and UHECRs

Radio galaxies with extended radio jets were classified into two categories by Fanaroff & Riley (1974): A population of high luminosity shows radio lobes at the outer edge of the jet, at kpc scales from the core, *Fanaroff Riley II objects, short FR-II*. The lower luminosity population, on the other hand, has radio knots distributed along the jet, the first knot being as close as ~ 3000 Schwarzschild radii from the central core, *Fanaroff Riley I objects,*

---

[1] For a first discussion of the Solar wind, see (Biermann, 1951), for shock acceleration in AGN see (Bednarz & Ostrowski, 1998, e.g.).

short FR-I. Both radio lobes and knots show non-thermal radio spectra, arising from electron acceleration at a shock front as first theoretically described by Fermi (1949, 1954). In analogy to processes in the creation of Galactic Cosmic Rays, protons are believed to be accelerated at those shock fronts in the same way as electrons. In particular, oblique shocks can be very efficient in particle acceleration, and use electric fields in shock-drift acceleration due to the Lorentz transformation of the magnetic fields in the proper frame, see (Hoffmann & Teller, 1950; Parker, 1958; Jokipii, 1987; Völk & Biermann, 1988; Biermann, 1993; Meli & Biermann, 2006; Meli et al., 2008).

1.1.1 *Unified model of FR-I galaxies and BL Lac objects*

In this paper, we consider FR-I galaxies as the sources of the UHECRs potentially observed by Auger. It is discussed by others (Taşcău, 2003; Cuoco & Hannestad, 2008; Halzen & O'Murchadha, 2008; Koers & Tinyakov, 2008; Kachelriess et al., 2008) that the nearby FR-I galaxy NGC5128, Centaurus A (Cen A in the following), is a good candidate to be responsible for a large fraction of the correlated events above 60 EeV. M 87 is another closeby candidate, see Biermann & Strittmatter (1987), which cannot contribute to a possible Auger correlation, since it is barely in Auger's field of view. The large number of more distant FR-I galaxies provide good candidates for the total Cosmic Ray flux above the ankle. Here, we discuss the morphology of FR-I type galaxies and how these can accelerate particles to the highest energies.

Figure 1 presents a schematic view of the model of FR-I galaxies that we use in this paper. On the x-axis, the rotational-symmetric part of the AGN is shown, while the y-axis represents the axis of rotational symmetry along the AGN jet. Both axes have logarithmic units. When the AGN jet is pointed towards Earth, the FR-I type galaxy is viewed as a BL Lac type object (Urry & Padovani, 1994, 1995), showing flat radio spectra, with an unresolved jet structure. When the AGN jet is viewed at an angle, the jet structure with radio knots distributed along the jet can be observed. In contrast to the more radio-luminous FR-II galaxies, FR-I type objects typically lack the observation of optical disks. While some of the FR-I type galaxies, such as M 87, clearly lack luminous accretion disks[2] and tori, many objects in this class may have accretion disks hidden behind the torus, provided that the torus is closed around the jet as indicated in Fig. 1, see (Falcke et al., 1995a). In this case, the jet-disk symbiosis model holds also for FR-I galaxies and the disk power scales with the radio luminosity.

_____

[2] They are likely to have radiatively inefficient accretion disks, typically for low accretion rates.
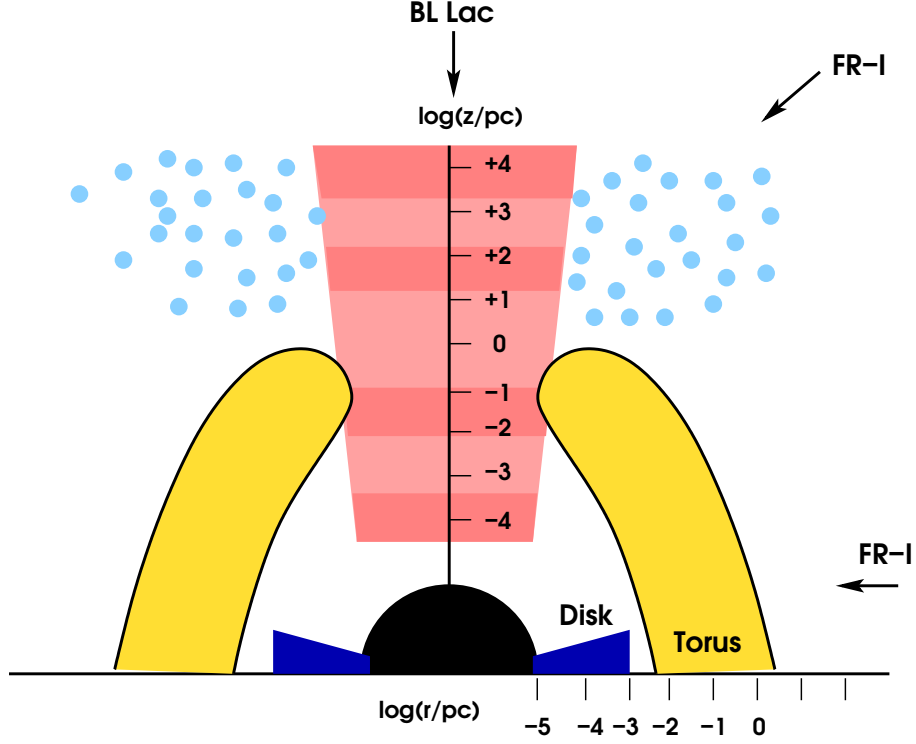
Fig. 1. Schematic figure of the class of FR-I galaxies with double-logarithmic scales. When the jet is pointed directly towards Earth, FR-I galaxies are classified as BL Lac objects. In this model, the torus will hide the accretion disk from view. In the case of a FR-I galaxy without torus, no radiatively efficient disk may be present.

1.1.2 Magnetic fields and shock structure in FR-I galaxies

The dependence of the magnetic field in these jets along the jet axis z_j is near $B \sim z_j^{-1}$ at large distances. However, in the inner region, the radial dependence is not certain. Here, we investigate the radial dependence of the magnetic field in order to determine the Cosmic Rays' maximum energy along the jet and in particular, at the innermost part of the jet.

Observations (Bridle & Perley, 1984, e.g.) suggest that the magnetic field runs as z_j^{-2} at first, since the radio polarization observation show that the magnetic field is parallel to the jet. By analogy to the solutions of div$\mathbf{B} = 0$ in a magnetic wind (Parker, 1958), the magnetic field locally shows a parallel component of $B_{||} \sim z_j^{-2}$. Further out, the magnetic field observations suggest that, just as in a wind, the magnetic field becomes perpendicular to the flow direction, and so $B \sim z_j^{-1}$. It is obvious that in a smooth wind, any component decreasing with z_j^{-1} will ultimately win over a component running as z_j^{-2}. As the equation of state is almost certainly relativistic (Falcke & Biermann, 1995; Falcke et al., 1995b, e.g.), the total pressure P depends on the density as $P \sim \rho^{4/3}$, while in a conical simple jet the density $\rho \sim z_j^{-2}$, giving in near equipartition (the magnetic field pressure running with the total pressure)

then $B \sim \sqrt{P(r)} \sim z_j^{-4/3}$.

However, repeated shock waves will reheat the material (see e.g. Sanders (1983), as well as Mach's original work in the 19th century, Mach & Wentzel (1884, 1885); Mach (1898)), and so we will assume that the Mach-number of the flow repeatedly comes back to the same value, while the jet flow velocity will stay approximately constant. Therefore going from crest to crest

$$P \sim \rho\,, \tag{1}$$

and so as a consequence

$$B \sim z_j^{-1}\,. \tag{2}$$

This is consistent with the concept that the jet stays approximately conical. This argument is independent of the orientation of the magnetic field, and so the radio polarization observations are not in contradiction, but need then an interpretation as arising from highly oblique shocks, which emphasize magnetic field components parallel to the shock surface. Highly oblique shocks are only possible for high Mach-numbers, which again is consistent.
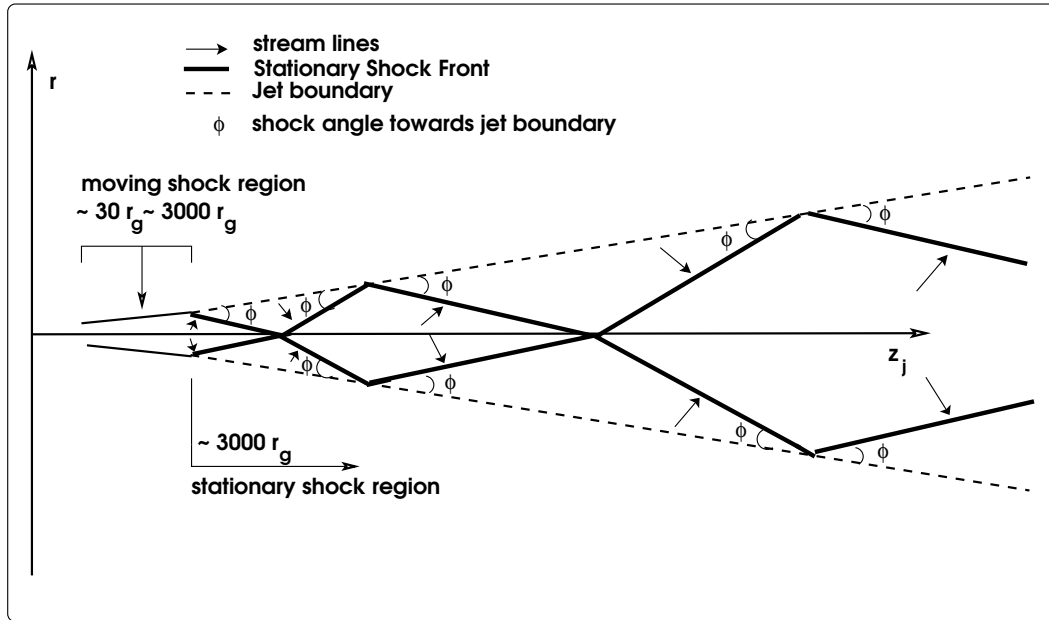

Fig. 2. Proposed conical shock structure in AGN jet.

As one check let us consider a system of repeated conical shocks, and ignore for simplicity the inner Mach disks as shown schematically in Fig. 2 (see also Sanders (1983)). Then we can see, that given a specific Mach-number at the initial flow formation there will be highly oblique shock waves, which will repeatedly reflect on the conical boundaries, and so produce a self-similar

pattern as long as the Mach-number keeps returning to near its initial value. A self-similar repeated structure with an ever increasing inner scale will result. This is precisely what is seen in jet structure at vastly discrepant spatial resolutions, like in the radio galaxy NGC6251 (Bridle & Perley (1984), and earlier papers). Further examples for such a shock structure are recent observations of BL Lacertae (Marscher et al., 2008) and the BL Lac type object S5 1803+784 (Britzen et al., 2008).

For those oblique, stationary shocks, it is likely that a mixture of sub- and superluminal shocks is present [3]. The proton spectra look very different when comparing the two cases. While superluminal spectra have maximum energies of around 10^5 GeV, subluminal shocks can reach energies up to the highest energies, i.e. $E_{\mathrm{max}} \sim 10^{21}$ eV, as shown by Meli et al. (2008).

Another consequence is that the magnetic field can be sufficiently high even far out to confine particles at the energies of UHECRs. As the magnetic field is anchored to the inner accretion rate, or its residual electric currents from an earlier accretion event, any magnetic field that decreases much faster than z_j^{-1} on the way out, will have difficulty to confine particles during their acceleration to the highest energies observed (Blandford, 1976; Blandford & Znajek, 1977; Blandford & Königl, 1979). Only a magnetic field which runs overall as $B \sim z_j^{-1}$ allows the magnetic field to be relatively high far out along the jet structure.

We conclude that the magnetic field then runs as $B \sim z_j^{-1}$ approximately.

1.1.3 Cosmic Ray acceleration in FR-I galaxies

Normally when considering where UHECRs can be accelerated, the spatial limit, or Hillas-limit, is invoked (Hillas, 1984). Using radio observations this suggests that radio hot spots of powerful Fanaroff-Riley II radio galaxies are very good bets: they are usually modelled as shocks (Meisenheimer et al., 1989), which can be shown to accelerate particles to near 10^{21} eV (Biermann & Strittmatter, 1987).

When using the information on the magnetic fields inferred from radio jets, their radio knots, and their hot spots, one typically finds 10^{-4} Gauss on kpc scales (Miley, 1980; Bridle & Perley, 1984). On the other hand, the maximum magnetic field close to the black hole, so on scales such as a few Schwarzschild radii, is given by 10^4 Gauss $(M_{BH}/10^8\, M_\odot)^{-1/2}$ (Shakura & Sunyaev, 1973; Blandford, 1976; Massi & Kaufman Bernadó, 2008). Therefore on radial scales

---

[3] The value of the angle between the magnetic field and the shock front normal determines whether a transformation into the Hoffmann-Teller frame ($\mathbf{E} = 0$) is possible (subluminal) or not (superluminal).

over a factor of 10^8 the magnetic field decreases by just this factor, quite indicative of a r^{-1} behavior. This was also used quite successfully by Blandford & Königl (1979). Therefore, we conclude that such a radial dependence of the overall magnetic field is well justified.

When estimating what the magnetic field might be in a jet, we have used the current accretion rate to indicate an estimate, connecting it to the accretion disk (Falcke & Biermann, 1995; Falcke et al., 1995b). This then gives usually a rather weak field in all cases when the overall activity is low, such as believed in BL Lac objects. And a weak field fails the Hillas test for UHECRs.

However, an alternative proposed by Blandford & Znajek (1977) is that the magnetic field is still quite high, from a prior accretion episode, and then the jet can be driven by a spin-down of the black hole. In this context the magnetic fields are higher, and even low power sources such as FR-I radio galaxies are possible sources of UHECRs (Duţan & Biermann, 2005, 2008).

In addition, the Lovelace limit (Lovelace, 1976) shows that the Poynting flux, a lower limit to the energy flux in a jet, is connected to the maximal energy of a particle confined in the jet by $L_{jet} = 10^{47}\,\mathrm{erg/s}\,(E_{\max}/10^{21}\mathrm{eV})^2$. Therefore a jet such as Cen A, estimated to carry probably around $10^{43}\,\mathrm{erg/s}$ (Whysong & Antonucci, 2003) cannot possibly accelerate particles - especially protons - to 10^{21} eV, at most it would seem, that 10^{19} eV is possible. This limit can be exceeded by three arguments This limit can be exceeded through three arguments: (a) The particles might be heavier than hydrogen. In this case, however, photo-disintegration will reduce the neutrino flux, see e.g. Hooper et al. (2005); Ave et al. (2005). Hence, we only consider protons in our calculations and this argument does not apply here. (b) Secondly and more importantly, Gallant & Achterberg (1999) show that the Lorentz factor of the shock in the local upstream frame enters squared. (c) Further, the jets might be intermittent, as strongly demonstrated by the radio galaxy Hercules A (Gizani & Leahy, 2003; Nulsen et al., 2005).

Therefore there is no a priori difficulty for FR-I radio galaxies to accelerate protons to near 10^{20} eV. With a magnetic field decreasing as z_j^{-1}, the Hillas spatial limit will give the same maximal proton energy at all radii.

1.2   Optical depth

We discuss the interaction of ultra high energy cosmic rays with three different targets along the AGN jet. We calculate the optical depth of interactions with the photon fields of the disk and the knots' synchrotron field. As a third possible target, we consider the interaction of UHECRs where the jet meets the torus (see Fig. 1).

(1) *Proton interactions with disk photons*

The optical depth for proton-photon interactions is given by the ratio of the length $l \approx z_j \cdot \theta$ and mean free path of the protons, $\lambda_{p\,\gamma_{\text{disk}}}$, in the jet in the disk's photon field $n_{\gamma_{\text{disk}}}$:

$$\tau_{p\,\gamma_{\text{disk}}} = \frac{l}{\lambda_{p\,\gamma_{\text{disk}}}} = z_j \cdot \theta \cdot n_{\gamma_{\text{disk}}} \cdot \sigma_{p\gamma}. \tag{3}$$

Here, $\sigma_{p\gamma} = 900\,\mu\text{barn}$ is the total cross section for the production of the Delta-resonance in proton-photon interactions (Biermann & Strittmatter, 1987).

To check on a realistic value for $\tau_{p\,\gamma_{\text{disk}}}$ we estimate the interaction probability as follows:

In an active galactic nucleus the accretion disk will produce a radiation field near to the nucleus. The accretion disk luminosity at full efficiency is given by

$$L_{\text{disk}} \approx \epsilon_{Edd} \cdot 10^{44}\,\text{erg/s}, \tag{4}$$

where $\epsilon_{Edd} < 1$ is the accretion rate relative to the maximum, the Eddington rate.

At some distance z_j along the jet, starting at about $3000\,r_g$, where $r_g = 1.5 \cdot 10^{12}\,M_{BH}/(10^7\,M_\odot)$ cm, the gravitational radius, we find stationary shock waves, see (Markoff et al., 2001, 2005) and also Marscher et al. (2008). Moving shock waves are expected to be present between $\sim 10\,r_s - 3000\,r_s$ as discussed in detail in Marscher et al. (2008). These shockwaves accelerate particles, and these particles, say protons, interact with the radiation field. The photon density is then given by

$$n_{\gamma_{\text{disk}}} = \frac{L_{\text{disk}}}{4\pi\,z_j^2\,c\cdot h\nu}, \tag{5}$$

where $h\nu$ is the typical photon energy, for which we adopt 20 eV, which is $h\nu = 3 \cdot 10^{-11}$ erg. Using $3000\,r_g$ as a reference radius, this expression can be rewritten as

$$n_{\gamma_{\text{disk}}} = 4 \cdot 10^{11}\,\epsilon_{Edd} \cdot \left(\frac{L_{\text{disk}}}{10^{44}\,\text{erg/s}}\right) \cdot \left(\frac{z_j}{3000\,r_g}\right)^{-2}\,\text{cm}^{-3}. \tag{6}$$

The optical depth across the jet, with the length across the jet as $\theta\,z_j$, is the given by

$$\tau_{p\,\gamma_{\text{disk}}} = 0.2 \cdot \epsilon_{Edd} \cdot \left(\frac{\theta}{0.1}\right) \cdot \left(\frac{z_j}{3000\,r_g}\right)^{-1} \cdot \left(\frac{L_{\text{disk}}}{10^{44}\,\text{erg/s}}\right), \tag{7}$$

8

decreasing linearly outwards. Since FR-I galaxies are not as efficient radiators as FR-II galaxies (see Section 1.1), the Eddington rate in the best case is $\epsilon_{edd} \sim 0.1$. Those FR-I sources with the torus close around the jet, the optical depth is therefore $\sim 2\%$. For other FR-I type objects, like M 87, where the accretion rate has decreased, the disk can be come very faint. This means changing from a radiative disk, (Shakura & Sunyaev, 1973; Novikov & Thorne, 1973, e.g.), to a radiatively inefficient disk, (Narayan & Yi, 1995, e.g.), and the optical depth will essentially be equal to zero.

(2) *Proton interactions with the synchrotron photon field in the jet*
   If protons interact with synchrotron photons in the same knot, the optical depth is given as $\tau_{p\,\gamma_{\mathrm{synch}}} \approx z_j \cdot \theta \cdot n^{rest}_{\gamma_{\mathrm{synch}}} \cdot \sigma_{p\gamma}$. The particle density of synchrotron photons, $n^{rest}_{\gamma_{\mathrm{synch}}}$, is given in the rest frame of the plasma and needs to be transformed into the observer's frame, $n^{obs}_{\gamma_{\mathrm{synch}}}$. Even if the shock is standing, the plasma is streaming with relativistic velocities along the jet, and so is the synchrotron photon field. The photon density observed at Earth is thus modified from the field that the interacting protons 'see' in the plasma's rest frame, see (Rybicki & Lightman, 1979, e.g.):

$$n^{rest}_{\gamma_{\mathrm{synch}}} = \Gamma^{-1} \cdot n^{obs}_{\gamma_{\mathrm{synch}}} \, . \tag{8}$$

Here, Γ is the boost factor of the streaming plasma relative to Earth. The photon density in the plasma's frame can be determined by assuming that the luminosity of a knot along the jet is a fraction $\epsilon_{\mathrm{knot}} \approx 0.1$ of the total synchrotron luminosity, $L_{\mathrm{synch}} \approx 10^{40}$ erg/s:

$$n^{obs}_{\gamma_{\mathrm{synch}}} \approx \frac{\epsilon_{knot} \cdot L_{\mathrm{synch}}}{4\pi \cdot z_j^2 \cdot c \cdot (h\nu)} \, . \tag{9}$$

The frequency of synchrotron photons is $\nu \sim 1$ GHz. Hence, the optical depth is

$$\tau_{p\,\gamma_{\mathrm{synch}}} \approx 0.9 \cdot \left(\frac{10}{\Gamma}\right)\left(\frac{\theta}{0.1}\right) \cdot \left(\frac{\epsilon_{\mathrm{knot}}}{0.1}\right)$$
$$\cdot \left(\frac{L_{\mathrm{synch}}}{10^{40}\,\mathrm{erg/s}}\right) \cdot \left(\frac{z_j}{3000\,r_g}\right)^{-1} \cdot \left(\frac{\nu}{1\,\mathrm{GHz}}\right)^{-1} \, . \tag{10}$$

Thus, for a relativistically streaming plasma of $\Gamma \sim 10$, optical depths around unity are expected. At the foot of the jet, where it is still very collimated, it can therefore be expected that a large fraction of the protons interacts before escaping, producing neutrinos. Farther outside in the jet, the size of the knots increases with the distance along the jet and the optical depth will decrease. So, even in the case of synchrotron radiation,

the main location of neutrino production is expected at the foot of the jet, while protons will be able to escape the source at larger distances from the core.

(3) *Proton interactions with the proton field*

For FR-I galaxies with closed tori, the outer edges of the jet will pass through the torus, at a distance of $z_j \sim 1 - 10$ pc from the central black hole. The column depth of the torus is[4] $X \sim 4 \cdot 10^{23}\,\mathrm{cm}^{-2}$. The proton-proton optical depth is therefore

$$\tau_{p\,p_{\mathrm{torus}}} = X \cdot \sigma_{pp} \approx 2 \cdot 10^{-3}\,, \tag{11}$$

with $\sigma_{pp} \approx 50$ mb. This interaction efficiency of 0.2% is small compared to the proton-photon optical depths discussed above. In addition, only the small fraction of all protons in the outer parts of the jet will interact (see Fig. 1). We conclude that proton-proton interactions can be neglected here[5].

To sum up, proton-photon interactions are the dominant source of high-energy neutrino production. Optical depths are around unity at the foot of the jet and decrease with the distance from the core. Therefore, we expect neutrino production in the first large shock at around $z_j \sim 3000\,r_g$.

1.3   Consequence for neutrino and Cosmic Ray emission

As a consequence of the high optical photon-proton optical depth close to the foot of FR-I jets, there has to be abundant neutrino production near that first shock, and that shock is in the already high speed relativistic flow. On the other hand, as we now suspect that there is lateral substructure in these relativistic flows (Gopal-Krishna et al., 2004; Lovelace, 1976, e.g.), things could be subtle as regards the specific beaming (Lind & Blandford, 1985, e.g.). This implies that the spatial conditions suffice for the production of 10^{12} GeV protons at the base of the jet, but losses due to proton interactions with the disk's photon field will take several powers of ten from that as we discuss in the following subsection. The ultra high energy particles we do observe probably receive their last energy increase at the last strong shock (see Biermann & Strittmatter

---

[4] For a discussion of the torus' column depth in AGN, see Zier & Biermann (2002) and references therein.

[5] This situation could change drastically for AGN with extremely high matter densities, i.e. GPS/CSS sources, where both proton-proton interactions and pion-proton interactions can occur O'Dea & Baum (1997). Those sources are not considered in this paper: due to their high proton-proton interaction rate, they are not good candidates for the observed charged Cosmic Ray spectrum. They could be very efficient neutrino emitters.

(1987)), since the optical depth decreases with the distance from the AGN core. Neutrino observations may have the spatial resolution to check on this.
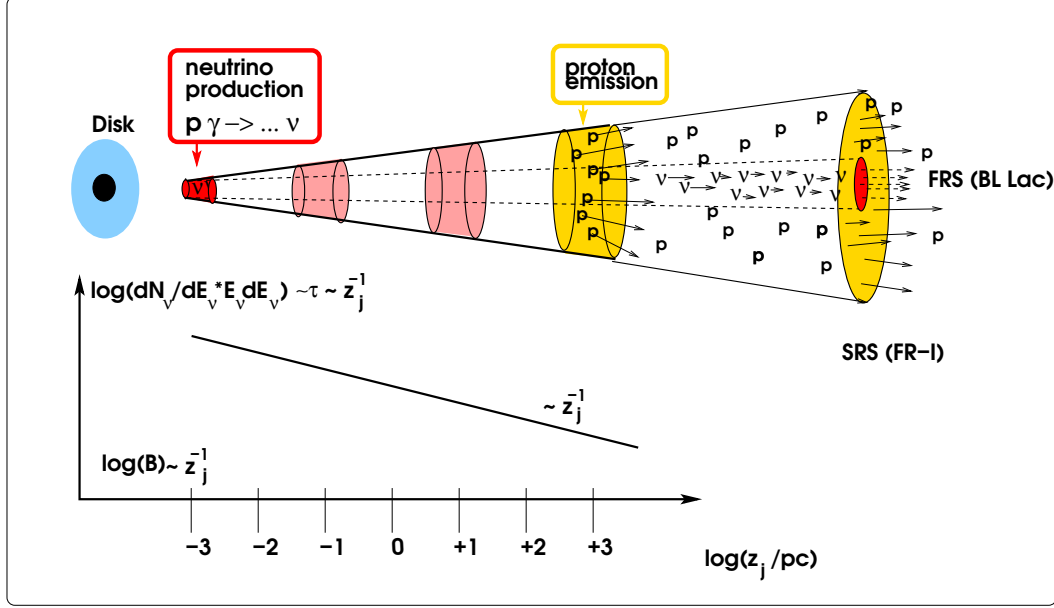

Fig. 3. Schematic figure of the AGN jet. The colored regions represent the emission regions. The detailed view of the shock structure discussed in Fig. 2 is not shown here, but it is assumed implicitly. While neutrino production happens in early, dense shocks, protons are more likely to come from the last shock, which is optically thin to proton-photon interactions. In this scenario, protons can be observed from FR-I galaxies, viewed from the side, and also from BL Lac objects, looking directly into the jet. Neutrino emission, on the other hand, is collimated and can only be observed from BL Lac objects.

The schematic view of this AGN model, showing the AGN jet with its shocks, is displayed in Fig. 3. Since neutrino production happens close to the foot of the AGN jet in a strongly accelerated reference system, the emission of neutrinos is beamed. The neutrino background due to active galactic nuclei has been estimated many times, usually in conjunction to the process of accelerating ultra high energy particles, see e.g. reviews by Gaisser et al. (1995); Halzen & Hooper (2002); Becker (2008). In particular, flat spectrum radio quasars (FSRQs), interpreted as FR-II sources with their jet pointing towards Earth, have been predicted to emit neutrinos by Mannheim et al. (1992); Atoyan & Dermer (2001, 2003); Becker et al. (2005). Further, one extensive work is by Bednarek & Protheroe (1999), who consider the acceleration of protons very close to the disk, up to distances of 10^{16} cm, and using a reconnection model for the acceleration, a process well studied in activity regions on the Sun. In our model, on the other hand, we discuss distances of about $3 \cdot 10^{3}$ gravitational radii, so for typical black hole masses of $10^{8} \, M_{\odot}$, so distances somewhat larger, about $4 \cdot 10^{16}$ cm, and adopt the point of view that shock wave acceleration is the dominant process. On the other hand, just as Bednarek & Protheroe (1999), we use the disk radiation as the photon field for interaction. Their fig-

11

ure 3a demonstrates the limit of such an approach: A typical disk temperature is of order $3 \cdot 10^4$ K (Malkan & Sargent, 1982; Donea & Biermann, 1996), or sometimes even higher, as also used in Bednarek & Protheroe (1999). They confirm that the optical depth is of order unity. However, there is one critical difference: In shock acceleration the energetic protons are isotropic in the co-moving frame, here moving with a Lorentz factor of order $10 - 30$, or perhaps even higher (Gopal-Krishna et al., 2007). So we do not have in our concept a proton moving rectilinearly straight out, but protons in a phase space distribution moving along with the relativistic jet flow (Falcke & Biermann, 1995). Hence, particle emission is beamed along the jet axis.

Neutrinos are therefore only observable from Earth if the jet points (almost) directly towards the observer. Since protons are likely to be produced in the last strong shock, AGN seen from the side also contribute to the flux of Cosmic Rays.

1.3.1 Flat Spectrum Radio Sources

As a consequence of the beamed neutrino emission, neutrinos correlated to the proton emission of radio galaxies can only be observed from flat spectrum radio sources (FRS), i.e. FR-I galaxies with their jet pointing towards Earth.

Most recently, the detection of a double-structure flare in optical and X-ray wavelengths from the flat spectrum radio source BL Lacertae was interpreted as the emission from particle acceleration in moving shock fronts very close to the central black hole. Then, when the plasma reaches the turbulent zone which marks the transition from moving to stationary shocks, a second synchrotron flare is seen from particle acceleration in the stationary shock, see Marscher et al. (2008) for details. During the first X-ray flare, > 200 GeV emission from BL Lacertae was detected by the MAGIC telescope (Albert et al., 2007). Marscher et al. (2008) explain this high-energy component by Inverse Compton scattering of the accelerated electrons with the synchrotron photons. An alternative explanation would be the production of very high-energy photons via photohadronic interactions. Here, charged and neutral pions are produced, the charged pions decaying to produce neutrinos and the neutral pions resulting in TeV photons. Thus, if the TeV signal is of hadronic nature, i.e. if it arises from π^0-decays, neutrinos are produced simultaneously, as also discussed by Mannheim et al. (1992).

1.3.2 Steep Spectrum Radio Sources

Steep spectrum radio sources are AGN seen from the side, often showing a detailed jet structure, with radio knots along the jets (FR-I galaxies) or radio lobes at the outer end of the jet. We predict that those sources are

weak neutrino sources, considering the model presented above: The beamed emission from the jet is not directed towards Earth and very strongly focused neutrino emission cannot be observed from Earth.

As for one of the brightest radio galaxies in the sky, Cen A, it will be possible to localize the origin of neutrinos within the source: the extension of Cen A is ten degrees on the sky, while the resolution of neutrino detection with IceCube will be around 1°. So, the flux of high energy neutrinos produced in each subsequent shock region will diminish with the distance from the black hole and the maximal energy will go up. However, as the jet of Cen A is not pointing near to the line of sight, we will see neutrinos only from secondary particles decay, after a primary charged particle has scattered in magnetic fields, near the boundary or outside the relativistic jet. In this paper, we will calculate the intensity of the neutrino signal connected to the possible correlation of UHECRs and the distribution of AGN as observed by Auger (Auger Collaboration, 2007, 2008).

2 Estimate of the Cosmic Ray flux from nearby sources

Recent Auger results (Auger Collaboration, 2007, 2008) indicate that at least 20 events above 57 EeV are correlated with the distribution of nearby AGN in the Véron-Cetty & Véron catalog, Véron-Cetty & Véron (2006), abbreviated VCV catalog in the following. The integrated exposure above 40 EeV is given as Exposure $= 9 \cdot 10^3$ km^2 yr sr and can be assumed to be the same above 57 EeV. Thus, the integral flux of UHECRs is

$$N(> E) = \frac{\#(events)}{\text{Exposure}} \tag{12}$$

and in this case

$$N(> 57\text{EeV}) = \frac{20}{9 \cdot 10^3}\text{km}^{-2}\text{yr}^{-1}\text{sr}^{-1} = 7 \cdot 10^{-21}\text{s}^{-1}\,\text{sr}^{-1}\,\text{cm}^{-2}\,. \tag{13}$$

If the flux is correlated to a single or few point source(s) rather than to many sources, the field of view (FoV) of Auger Ω_{Auger} has to be taken into account in combination with the declination of the sources $\omega_{\text{source}}(\delta)$, as discussed in the approaches of Cuoco & Hannestad (2008); Halzen & O'Murchadha (2008); Koers & Tinyakov (2008). As opposed to those models, we calculate the diffuse contribution as a conservative estimate, based on a detailed model concerning the physics of the AGN jet.

Based on the correlation claimed by Auger, we assume in the following calculation that these 20 events come from AGN in the supergalactic plane (SGP).

If the source population for the origin of the calculation is verified to be radio galaxies, it is likely that even more than 20 events come from AGN, since the VCV catalog is not complete.

The differential flux from the SGP can be assumed to follow a power-law,

$$\frac{dN_{\mathrm{CR}}}{dE_{\mathrm{CR}}}\bigg|_{SGP} = A_{\mathrm{SGP}} \cdot E_{\mathrm{CR}}^{-p} \,. \tag{14}$$

Here, the cosmic ray energy E_{CR} is given in the laboratory frame at Earth. In all following calculations, energies E are in the laboratory frame at Earth, energies $E^{\mathrm{source}} = (1+z) \cdot E$ are given in the laboratory frame at the source and $E' = E^{\mathrm{source}}/\Gamma = E \cdot (1+z)/\Gamma$ represent the energy in the shock rest frame, with Γ as the bulk Lorenz factor of the shock and z as the cosmological redshift of the source. All calculations are done in the way that energies have units of $[E] = [E^{\mathrm{source}}] = [E'] = \mathrm{GeV}$. The normalization factor A_{SGP} can be determined by using Equ. (13) and comparing it to the integral form of Equ. (14):

$$N(> E_{\mathrm{Auger}}^{\mathrm{min}}) = \int\limits_{E_{\mathrm{Auger}}^{\mathrm{min}}} dE_{\mathrm{CR}} \frac{dN_{\mathrm{CR}}}{dE_{\mathrm{CR}}} = A_{\mathrm{SGP}} \int\limits_{E_{\mathrm{Auger}}^{\mathrm{min}}} E_{\mathrm{CR}}^{-p} \, dE_{\mathrm{CR}}$$
$$\approx A_{\mathrm{SGP}} \cdot (p-1)^{-1} (E_{\mathrm{Auger}}^{\mathrm{min}})^{-p+1} \tag{15}$$

Thus, the normalization factor A_{SGP} can be calculated to be

$$A_{\mathrm{SGP}} = N(> E_{\mathrm{Auger}}^{\mathrm{min}}) \cdot (p-1) \cdot (E_{\mathrm{Auger}}^{\mathrm{min}})^{p-1} \tag{16}$$

with $E_{\mathrm{Auger}}^{\mathrm{min}}$ in units of GeV and $[A_{\mathrm{SGP}}] = \mathrm{GeV}^{-1}\mathrm{s}^{-1}\,\mathrm{sr}^{-1}\,\mathrm{cm}^{-2}$. The spectral index p of UHECRs is observed to be 2.7. However, stochastic shock acceleration itself results in a spectrum with a spectral index of 2.3 or even flatter, see e.g. papers by Bednarz & Ostrowski (1998); Kardashev (1962); Baring (2004) or Meli et al. (2007, 2008). The steep observed spectrum may be due to the fact that there is a distribution of maximum energies or due to propagation effects. Therefore, we use index values of $p = 2.3$ and $p = 2.0$ for the sources of UHECRs in the SGP. For a threshold energy of 57 EeV and an integral flux of $7 \cdot 10^{-21}\mathrm{s}^{-1}\,\mathrm{sr}^{-1}\,\mathrm{cm}^{-2}$, the numerical value of the normalization constant is

$$A_{\mathrm{SGP}} = \begin{cases} 9 \cdot 10^{-7}\,\mathrm{GeV}^{-1}\mathrm{s}^{-1}\,\mathrm{sr}^{-1}\,\mathrm{cm}^{-2} & \text{for } p = 2.3 \\ 4 \cdot 10^{-10}\,\mathrm{GeV}^{-1}\mathrm{s}^{-1}\,\mathrm{sr}^{-1}\,\mathrm{cm}^{-2} & \text{for } p = 2.0 \,. \end{cases} \tag{17}$$

Figure 4 shows the observed cosmic ray spectrum at UHEs, weighted with $E_p^{2.7}$. Data are from the HiRes (Abbasi et al., 2008b) and Auger (Abraham et al.,
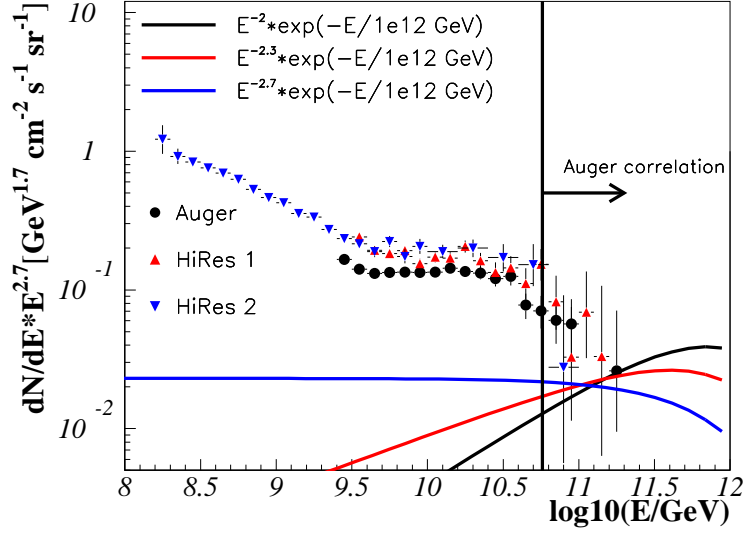
Fig. 4. Differential UHECR spectrum weighted with $E^{-2.7}$ - measurements from Auger (circles), (Abraham et al., 2008), and HiRes-I and HiRes-II (triangles), (Abbasi et al., 2008b). The data from the two different experiments are comparable when considering small systematics in the energy measurements (Roth, 2008). The differential flux from the supergalactic plane calculated for E^{-2} (black line), $E^{-2.3}$ (red line) and $E^{-2.7}$ (blue line). An exponential cutoff was applied at 10^{12} GeV.

2008) experiments. The flux from the supergalactic plane as calculated above is indicated as the blue ($p = 2.7$), red ($p = 2.3$) and black ($p = 2.0$) lines. The three indices represent different models for the description of Cosmic Ray production and propagation following the theoretical results of Berezinsky et al. (2006) in the case of $p = 2.7$, the work of (Bednarz & Ostrowski, 1998) for $p = 2.3$, using parallel shocks, and the results of Meli et al. (2007, 2008) for oblique shock conditions ($p = 2$). The energy flux can be calculated from the differential spectrum as

$$j(E_{\text{th}}) = \int_{E_{\text{th}}} E \, dN/dE \, dE \, .\tag{18}$$

The total energy flux measured in cosmic rays above $E_{\text{th}} = 10^{9.5}$ GeV is approximately

$$j_{\text{tot-CR}} \approx 10^{-7} \, \text{GeVs}^{-1} \, \text{sr}^{-1} \, \text{cm}^{-2} \, .\tag{19}$$

The corresponding energy flux from the supergalactic plane can be calculated by using the same energy threshold and the differential spectrum determined above:

15

$$
j_{\mathrm{SGP-CR}} = \begin{cases} \frac{A_{\mathrm{SGP}}}{p-2} \cdot E_{\mathrm{th}}^{-p+2} & \text{for } p \neq 2 \\ A_{\mathrm{SGP}} \cdot \ln(E_{\mathrm{max}}/E_{\mathrm{th}}) \end{cases} \tag{20}
$$

$$
\approx \begin{cases} 4 \cdot 10^{-9}\,\mathrm{GeVs^{-1}\,sr^{-1}\,cm^{-2}} & \text{for } p = 2.3 \\ 9 \cdot 10^{-10}\,\mathrm{GeVs^{-1}\,sr^{-1}\,cm^{-2}} & \text{for } p = 2.0 \end{cases}. \tag{21}
$$

Here, a maximum energy of $E_{\mathrm{max}} = 10^{10.5}$ GeV was used, taking into account the GZK cutoff. This implies that about 1% of the total cosmic ray flux above the ankle is made up by sources in the supergalactic plane.

3   Neutrino flux estimate from Auger measurements

With protons being accelerated in AGN jets, neutrinos can be produced in photohadronic interactions (see e.g. Becker (2008) for a review),

$$
p\,\gamma \to \Delta^+ \to \begin{cases} \pi^0\,p \to \gamma\,\gamma\,(p) & 2/3 \text{ of the cases} \\ \pi^+\,n \to \mu^+\,\nu_\mu\,(n) \to \overline{\nu}_\mu\,\nu_e\,\nu_\mu\,(e^+\,n) & 1/3 \text{ of the cases} \end{cases}. \tag{22}
$$

Here, the branching ratio for charged pion production is $1/3$. About $1/2$ of the pion's energy goes into the sum of muon and anti-muon neutrinos (Notation: $\nu := \nu_\mu + \overline{\nu}_\mu$). In addition, neutrinos oscillate on their way to Earth from a ratio of

$$
(\nu_e,\, \nu_\mu,\, \nu_\tau)|_{\mathrm{source}} = (1:2:0) \text{ to } (\nu_e,\, \nu_\mu,\, \nu_\tau)|_{\mathrm{Earth}} = (1:1:1), \tag{23}
$$

see e.g. Stanev (2004) and references therein. Given an optical depth $\tau_{p\gamma}$ for the production of the Delta-resonance, the total neutrino energy flux j_ν, radiated in the solid angle Ω_ν, $(\Omega_\nu\, j'_\nu) = \int E'_\nu\, dN_\nu/dE'_\nu\, dE'_\nu$, and the total proton energy flux, focused within the solid angle Ω_{CR}, $(\Omega_{\mathrm{CR}}\, j'_p) = \int E_p\, dN_p/dE_p\, dE_p$, both given in the shock rest frame, are therefore connected as

$$
(\Omega_\nu \cdot j'_\nu) = \tau_{p\gamma} \cdot \frac{1}{3} \cdot \frac{1}{2} \cdot \frac{1}{2} \cdot (\Omega_{\mathrm{CR}}\, j'_p) = \frac{\tau_{p\gamma}}{12} \cdot (\Omega_{\mathrm{CR}}\, j'_p). \tag{24}
$$

The optical depth will be set to $\tau_{p\gamma} = 1$ in the following calculations (see Section 1 for a detailed discussion). This correlation can be used to estimate the neutrino flux to be expected from the supergalactic plane, given the proton flux at Earth as in Equations (14) and (16). First, we need to connect the energy flux in the shock rest frame and the one measured at Earth.

3.1 The energy flux

The diffuse energy flux of a certain particle species is given in terms of the energy spectrum at Earth as described in Equ. (18). In terms of the single source spectrum, it can be written as

$$j = \int\limits_{E^{\text{source}}} \int\limits_{z_{\min}}^{z_{\max}} \int\limits_{L_{\min}}^{L_{\max}} dE^{\text{source}}\, dz\, dL\, E^{\text{source}} \frac{dN}{dE^{\text{source}}} \cdot \frac{1}{4\pi\, d_L^2} \cdot \frac{d^2n}{dV\, dL} \cdot \frac{dV}{dz}. \tag{25}$$

Here, we are taking into account the following facts:

(a) Each source contributes with $E^{\text{source}}\, dN/dE^{\text{source}}\, dE^{\text{source}}$.

(b) The flux of each source decreases with $4\pi\, d_L^2$, where d_L is the source's luminosity distance.

(c) The source number per comoving volume dV/dz and per luminosity interval, $dn/dV/dL$ - for protons, we use the radio luminosity function of FR-I galaxies, observed neutrinos are only produced in FRS.

(d) Sources up to a redshift $z_{\max}$, with an absolute upper limit of 0.03 as the outskirts of the supergalactic plane contribute to the energy flux, both for neutrino and for proton sources. The minimum redshift is given by the distance of the closest plausible source, Cen A, at $z_{\min}^{\text{CR}} = 0.0008$ in the case of FR-I galaxies [6] (CR sources), and Perseus A at $z_{\min}^{\nu} = 0.018$ in the case of FRS (Neutrino sources).

(e) The luminosity integration limits for AGN have been chosen to match the observed distribution of FR-I galaxies, $L_{\min} = 10^{40}$ erg/s and $L_{\max} = 10^{44}$ erg/s. This applies for FRS as well, as these are generally believed to be a sub-class of FR-I galaxies.

As we would like to compare the diffuse energy flux at Earth to the energy flux in the shock rest frame, we use $E^{\text{source}} = \Gamma \cdot E'$ and receive

$$j = \frac{\Gamma}{4\pi} \cdot \int\limits_{E'} dE'\, E' \frac{dN}{dE'} \cdot \int\limits_{z_{\min}}^{z_{\max}} \int\limits_{L_{\min}}^{L_{\max}} dz\, dL \frac{1}{d_L^2} \cdot \frac{d^2n}{dV\, dL} \cdot \frac{dV}{dz} \tag{26}$$

$$= \frac{\Gamma}{4\pi} \cdot j' \cdot n, \tag{27}$$

---

[6] Cen A is located at a distance of 3.5 Mpc which corresponds to a corrected redshift of 0.00083 for a cosmology of $\Omega_m = 0.3$, $\Omega_\Lambda = 0.7$ and $h_0 = 0.7$, using approximate values from most recent WMAP-5year results (Komatsu et al., 2008). The apparent, measured redshift is much higher than the actual cosmological one, due to the gravitational influence of the Great Attractor on nearby sources.

with

$$n = \int\limits_{z_{\min}}^{z_{\max}} \int\limits_{L_{\min}}^{L_{\max}} dz \, dL \frac{1}{4\pi \, d_L^2} \cdot \frac{d^2 n}{dV \, dL} \cdot \frac{dV}{dz} \, . \tag{28}$$

Inserting Equ. (27) into Equ. (24) for both neutrinos and protons, we have

$$j_\nu = \frac{1}{12} \frac{\Gamma_\nu}{\Gamma_{\rm CR}} \cdot \frac{\Omega_{\rm CR}}{\Omega_\nu} \cdot \frac{n_\nu}{n_{\rm CR}} \cdot j_{\rm CR} \, . \tag{29}$$

3.2 Discussion of parameters

- **Cosmic ray energy flux at Earth**

  The proton energy flux can be written as

  $$j_{\rm SGP-CR} = A_{\rm SGP} \int dE_{\rm CR} E_{\rm CR}^{-p+1} \tag{30}$$

  $$= A_{\rm Auger} \cdot \begin{cases} (p-2)^{-1} \cdot (E_{\rm CR}{}^{\min})^{-p+2} & \text{for } p \neq 2 \\ \ln\left(\frac{E_{\rm CR}^{\max}}{E_{\rm CR}^{\min}} \right) & \text{for } p = 2 \end{cases} \tag{31}$$

  $$= \frac{p-1}{p-2} \cdot N(> E_{\rm Auger}^{\min}) \cdot (E_{\rm Auger}^{\min})^{p-1} \cdot (E_{\rm CR}^{\min})^{-p+2} \text{ for } p \neq 2 \, . \tag{32}$$

  The proton energy is given in units of GeV and $[A_p] = \text{GeV}^{-1}\text{s}^{-1}\,\text{sr}^{-1}\,\text{cm}^{-2}$. For protons, the lower energy threshold is given as the proton mass boosted by $\Gamma_{\rm CR}$, $E_{\rm CR}^{\min} = m_p \approx \Gamma_{\rm CR} \cdot 1$ GeV.

- **Neutrino energy flux at Earth**

  It is assumed that the neutrino spectrum traces the proton spectrum,

  $$\frac{dN_\nu}{dE_\nu} = A_\nu \cdot E_\nu^{-\alpha_\nu} \tag{33}$$

  with $\alpha_\nu \approx p$, E_ν in units of GeV and $[A_\nu] = \text{GeV}^{-1}\text{s}^{-1}\,\text{sr}^{-1}\,\text{cm}^{-2}$. The neutrino energy flux can then be expressed as

  $$j_\nu = A_\nu \int\limits_{E_\nu^{\min}} dE_\nu E_\nu^{-\alpha_\nu+1} \tag{34}$$

  $$= A_\nu \begin{cases} (\alpha_\nu - 2)^{-1} \cdot (E_\nu^{\min})^{-\alpha_\nu+2} \approx 10 \cdot \Gamma_\nu^{-\alpha_\nu+2} & \text{for } \alpha_\nu \neq 2 \\ \ln\left(\frac{E_{\max}^\nu}{E_{\min}^\nu} \right) & \text{for } \alpha_\nu = 2 \, . \end{cases} \tag{35}$$

  The lower energy threshold of one fourth of the pion mass, boosted by Γ_ν, $E_\nu^{\min} = \Gamma_\nu \cdot m_\pi/4 = \Gamma_\nu \cdot 0.035$ GeV, dominates and the upper energy

18

threshold can be neglected in the case of $\alpha_\nu \neq 2$. For $\alpha_\nu = 2$, the logarithm for neutrino energy equals approximately the one for proton energies and the factors cancel in the end.

Concerning the threshold energies and spectral behavior of the flux, our model differs from other approaches by Cuoco & Hannestad (2008); Halzen & O'Murchadha (2008); Koers & Tinyakov (2008) in the sense that we assume proton interactions with the photon field from the disk and from the synchrotron radiation in the jet. In the models of Cuoco & Hannestad (2008); Halzen & O'Murchadha (2008); Koers & Tinyakov (2008), X-ray photons are assumed to interact with the protons in the sources, which results in a broken power-law behavior when calculating the neutrino flux. The reason is that the optical depth for proton-photon interaction changes with energy, and this change happens at a neutrino energy of around $\sim 10^6$ GeV for X-ray photons. In the case of optical or radio photons, the break is at very low energies, so that it is not relevant for our calculations. Thus, the neutrino flux calculated here follows a single power-law just as the proton spectrum does.

- *Lorentz factor*

  As neutrinos come from early shocks near the black hole, the beaming factor is typically stronger than for protons from late, outer shocks. We will assume in the following that the boost factor for neutrino production is a factor of ~ 3 higher than for protons,

  $$\frac{\Gamma_\nu}{\Gamma_{\mathrm{CR}}} \approx 3 \,. \tag{36}$$

- *Solid angle*

  We assume in the following that $\Omega \propto \theta^2 \propto 1/\Gamma^2$ as the typical opening angle for relativistic sources. In particular, $\Omega_\nu \approx 1/\Gamma_\nu^2$ and $\Omega_{\mathrm{CR}} \propto 1/\Gamma_{\mathrm{CR}}^2$.

- *Redshift dependence*

  The redshift dependence of the neutrino energy flux is given as

  $$n_\nu = \int\limits_{z_{0.018}}^{z_{\mathrm{max}}^\nu} \int\limits_{L_{\mathrm{min}}}^{L_{\mathrm{max}}} dz\, dL \frac{1}{4\pi\, d_L^2} \cdot \left. \frac{d^2 n}{dV\, dL}\right|_{\mathrm{FRS}} \cdot \frac{dV}{dz} \,. \tag{37}$$

In a first approach, we will calculate the total diffuse neutrino flux from the supergalactic plane and use $z_{\mathrm{max}}^\nu = 0.03$ as the upper integration limit, see also Das et al. (2008). The radio luminosity function for flat spectrum radio sources, $d^2 n/dV/dL|_{\mathrm{FRS}}$, determined by Dunlop & Peacock (1990). The authors do not distinguish between the high- and low-luminosity sources,

19

so both FR-II type objects ("FSRQs") and FR-I ("BL Lacs") are included. Since the low-luminosity part of the sources makes up most of the population, we neglect the contribution of FSRQs here and interpret this function of flat spectrum radio sources (FRS) as an approximation of the FR-I component of blazars.

As discussed before, neutrino emission is beamed and originates from FRS only. For protons, all FR-I galaxies contribute:

$$
n_{\mathrm{CR}} = \int\limits_{0.0008}^{z_{\max}^{\mathrm{CR}}} \int\limits_{L_{\min}}^{L_{\max}} dz\, dL \frac{1}{4\pi\, d_L^2} \cdot \left.\frac{d^2 n}{dV\, dL}\right|_{\mathrm{FR-I}} \cdot \frac{dV}{dz} \,.
\tag{38}
$$

The radio luminosity function of FR-I galaxies is given in Willott et al. (2001). As the Auger correlation at most reveals a general correlation between the distribution of AGN and cosmic rays, the exact number of sources is not known. Note that the extension of sources goes with the distance squared rather than with the total volume due to the disk-like structure of the SGP, see Cavaliere & Menci (1997). This is compensated by using the volume integration for both the neutrino and the Cosmic Ray sources: The relevant ratio n_ν/n_{CR} gives the correct result.

Figure 5 shows how the ratio n_ν/n_{CR} depends on the maximum redshift of contributing sources to the observed correlation. The more sources contribute, the larger n_{CR} and the smaller the ratio. The most conservative assumption is to assume that all sources in the supergalactic plane contribute to the correlation, $z_{\max}^{\mathrm{CR}} = 0.03$, see also Das et al. (2008). The most optimistic assumption is that only the nearest sources contribute, $z_{\max}^{\mathrm{CR}} = 0.001$. Thus, the values lie between

$$
0.1 < \frac{n_\nu}{n_{\mathrm{CR}}} < 5 \,.
\tag{39}
$$

3.3 The diffuse neutrino flux from the supergalactic plane

Inserting the results from Section 3.2 into Equ. (29) yields a numerical value for the neutrino normalization constant,

$$
\begin{aligned}
A_\nu =\ & \frac{n_\nu}{n_{\mathrm{CR}}} \cdot \left(\frac{\Gamma_\nu}{\Gamma_{\mathrm{CR}}}\right)^{5-p} \cdot \frac{\tau_{p\gamma}}{12} \\
& \cdot N(> E_{\mathrm{CR}}^{\min}) \cdot (p-1) \cdot (\frac{m_\pi}{4})^{p-2} \cdot (E_{\mathrm{Auger}}^{\min})^{p-1} \,,
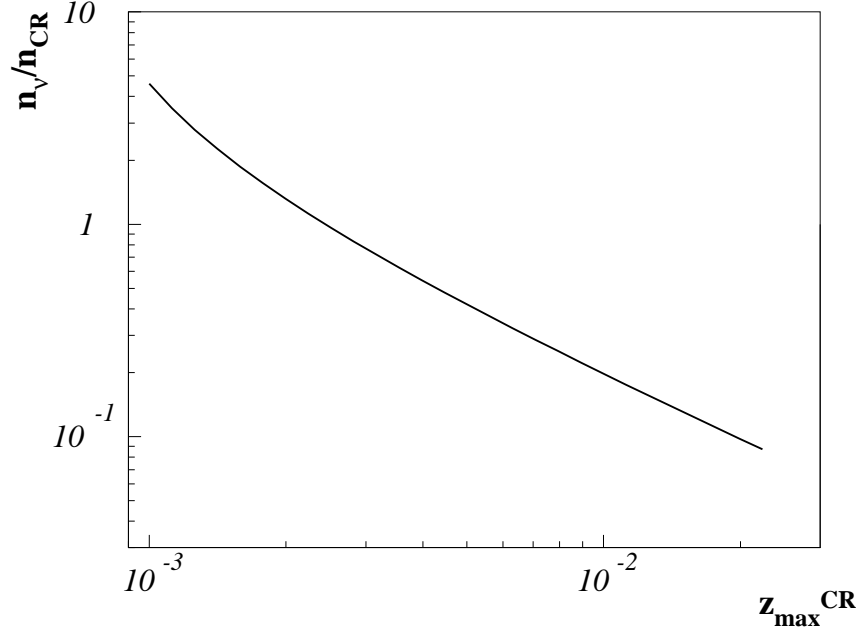\end{aligned}
\tag{40}
$$

20

Fig. 5. Redshift factor n_ν/n_{CR} for with variable maximum redshift for n_{CR}. If only very nearby sources are responsible for the correlation of UHECRs with the distribution of AGN, $z_{\max}^{CR}$ can be as small as $z_{\max}^{\mathrm{CR}} = 0.001$. If the correlation comes from the entire distribution of sources, the maximum redshift is given by the extension of the supergalactic plane, $z_{\max}^{\mathrm{CR}} = 0.03$. The minimum redshift for integration is taken to be $z_{\min}^{\mathrm{CR}} = 0.0008$ for the cosmic ray factor, using Cen A as the closest contributing source, and the neutrino factor has $z_{\min}^{\nu} = 0.018$ as Perseus A as the closest contributing source. The maximum redshift for neutrinos is taken to be $z_{\max}^{\nu} = 0.03$.

where $\tau_{p\gamma} = 1$ was assumed, as discussed in more detail in Section 1.

The neutrino flux for an $E^{-2}-$ and an $E^{-2.3}-$ shaped spectrum is shown in Fig. 6, assuming that the Auger correlation is caused by all sources up to $z_{\max}^{\mathrm{CR}} = 0.03$. The neutrino flux is higher at lower energies for the steeper spectrum $E_\nu^{-2.3}$. The reason is that the normalization is done at Auger's threshold energy. If the spectrum is steep $\sim E_\nu^{-2.3 \to -2.7}$, the energy content at lower energies is higher. If the spectrum is very flat (e.g. E_ν^{-2}), the contribution at energies lower than $E_{\mathrm{CR}}^{\min}$ is also lower (see Fig. 7). If the spectrum flattens towards smaller energies, this reduces the normalization as well.

The numerical value of the neutrino normalization constant for an $E_\nu^{-2}-$spectrum is

$$
A_\nu = \begin{cases} 1.4 \cdot 10^{-10}\,\mathrm{GeVs^{-1}\,sr^{-1}\,cm^{-2}} & \text{for } z_{\max}^{\mathrm{CR}} = 0.03 \\ 5.0 \cdot 10^{-9}\,\mathrm{GeVs^{-1}\,sr^{-1}\,cm^{-2}} & \text{for } z_{\max}^{\mathrm{CR}} = 0.002 \,. \end{cases} \tag{41}
$$

21

The expected neutrino flux is about a factor of 35 higher if the closest AGN produce the correlation of cosmic rays and AGN.
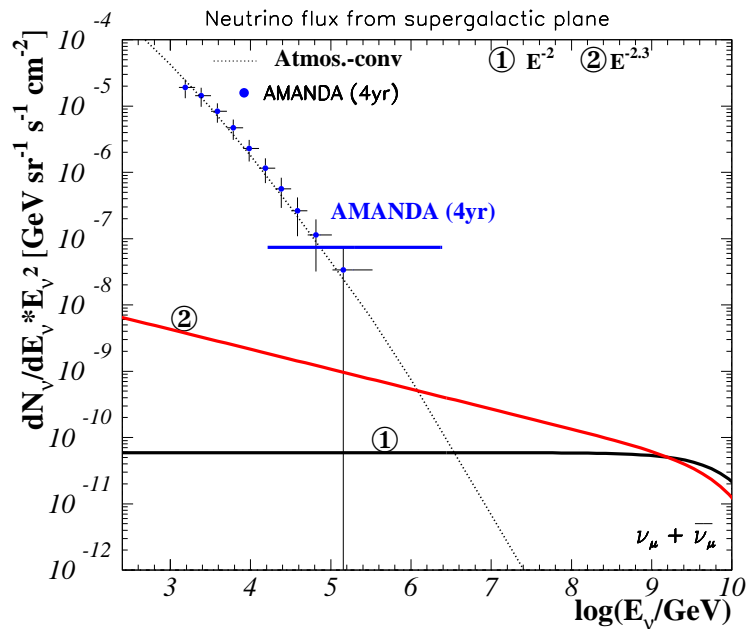

Fig. 6. Diffuse neutrino flux from the supergalactic plane, based on Auger data. The black line, labeled ①, is based on an E^{-2} spectrum, the red line, labeled ②, is calculated using $E^{-2.3}$. AMANDA data are taken from Münich et al. (2007) and the AMANDA limit is given in Achterberg et al. (2007).
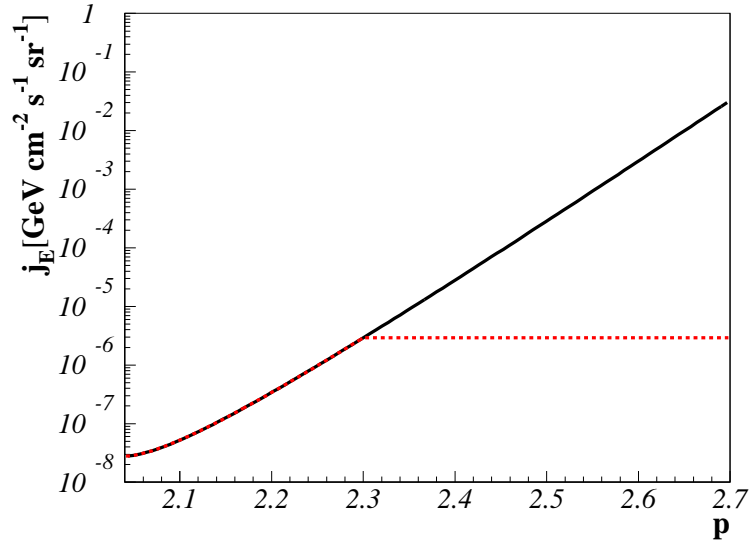
Fig. 7. Proton energy density, based on an E^{-p} spectrum (black line). Assuming that a spectrum steeper than $E^{-2.3}$ at the highest energies actually approaches $E^{-2.3}$ at low energies, the energy density saturates at $p = 2.3$ (red, dashed line). Still, there is a difference in the energy density of two orders of magnitude between assuming an E^{-2} spectrum and an $E^{-2.3}$ spectrum.

The total, extragalactic neutrino flux can be calculated by integrating up the neutrino flux redshift dependence up to $z^{\nu}_{\max} = 7$, where the first active galaxies are believed to contribute, see Bouwens & Illingworth (2006); Iye et al. (2006). The result is shown in Fig. 8. Here, we use the conservative assumption that sources up to $z^{\mathrm{CR}}_{\max} = 0.03$ contribute to the correlation between cosmic rays and the distribution of AGN. For an $E^{-2}-$shaped spectrum (black, horizontal, solid line), the flux is about a factor of 10 higher than the prediction made in Becker et al. (2005), where the jet-disk symbiosis model was used to estimate the neutrino flux from FSRQs. Since we normalize the AGN spectrum at the highest energies, a steeper neutrino spectrum (e.g. $E^{-2.3}$, red, solid line) leads to a higher flux at low energies. Although the figure seems to indicate that an $E^{-2.3}-$ flux is already excluded by AMANDA data, it should be noted that the limit is derived for an $E^{-2}-$ shaped spectrum. To be able to exclude the $E^{-2.3}-$ spectrum, the limit needs to be calculated for the same spectral behavior, see (Becker et al., 2006; Achterberg et al., 2007).
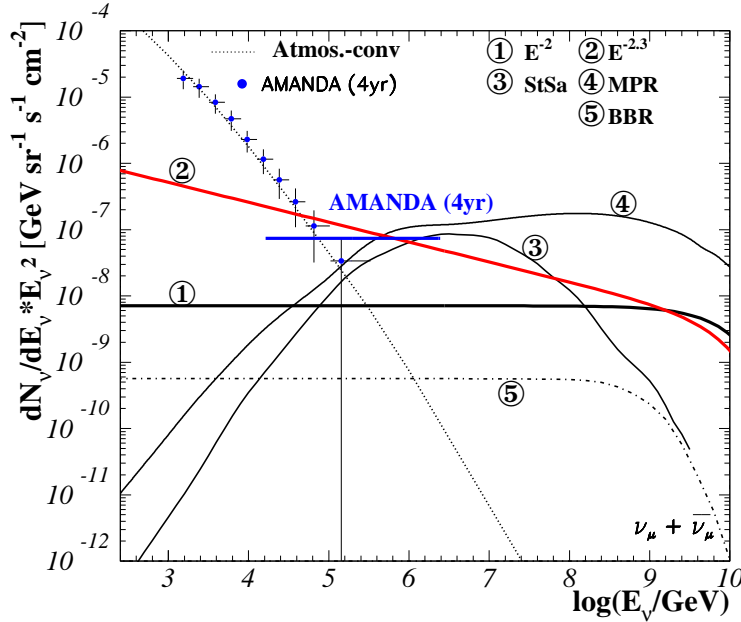

Fig. 8. Diffuse neutrino flux from flat spectrum radio sources up to $z < 7$. The black line, labeled ①, is based on an E^{-2} spectrum, the red line, labeled ②, is calculated using $E^{-2.3}$. The lines labeled ③ and ④ are shown for comparison, from Stecker (2005) and Mannheim et al. (2001), respectively. The two models use the high-energy component from AGN, $E_{\gamma} > \mathrm{MeV}$, to calculate the correlated neutrino flux. AMANDA data are taken from Münich et al. (2007) and the AMANDA limit is given in Achterberg et al. (2007). The dashed line, labeled ⑤, shows the prediction of the neutrino flux from FSRQs as calculated in Becker et al. (2005).

Neutrino flux calculations typically bear three significant sources of uncertainties, the first one being in the total normalization of the spectrum, the second one lying in the uncertainty of the spectral behavior. The third one is the maximum neutrino energy of the source class. Both quantities always rely on the internal properties of the source class, which are typically poorly determined. This is true in general and does not only apply to these calculations. Here, we explain how these calculations are effected by the uncertainties.

(1) *The normalization*
   The uncertainty in the normalization of neutrino spectra has three main components: the *measured spectrum* used to normalize the neutrino flux, the *optical depth* in the sources and the *opening angle* of neutrino and proton emission.
   The correlation of the highest energy Cosmic Rays with the VCV catalog is based on 20 events. These statistics need to be enhanced in order to achieve a more precise prediction of the actual Cosmic Ray flux from the source class. In addition, the composition of the spectrum is important for the neutrino flux, since protons produce more neutrinos than heavy nuclei do.
   Secondly, the optical depth of the sources depends on the size of the acceleration region, on the luminosity, on the boost factor and on the photon density in the acceleration region. Those properties are known for a few single objects, but they can vary with the source and also with time in a given source.
   The ratio of opening angles of proton and neutrino emission is conservatively taken to be ~ 3. However, the real ratio clearly depends on the properties of the single AGN, on the location of the first and last shocks.

(2) *The spectral index*
   Depending on the orientation of the shock towards the magnetic field and the boost factor, the spectral behavior can vary. For parallel shocks, a spectral behavior of $E^{-2.3}$ is expected as discussed by Bednarz & Ostrowski (1998). If using large angle scattering instead of pitch angle scattering for parallel shocks, particle spectra of up to $E^{-1.5}$ can be obtained Stecker et al. (2007). For oblique, subluminal shocks, the spectra behave as $E^{-2.0 \rightarrow -1.5}$, depending on the boost factor, as discussed by Meli et al. (2008).

(3) *Maximum energy*
   As discussed before, the maximum energy of the protons, and hence of the neutrinos, depends on intrinsic quantities like the magnetic field, boost factor and the disk luminosity.

So, to conclude, the importance of large volume neutrino detectors is enhanced by the fact that protons or high-energy photons cannot give unambiguous evidence for the spectral index, nor for the strength of the neutrino flux. In order to identify the nature of the shocks in not only AGN, but any Galactic or extragalactic accelerator, neutrinos are essential. In this paper, we predict the $r$egion of neutrino production in AGN jets. We predict that flat spectrum radio sources should be dominant. This can easily be tested by future experiments like IceCube and Km3NeT.

4 Summary and implications

In this paper, we present a model for Cosmic Ray and neutrino emission from active galactic nuclei. A first evidence for the correlation of the observed UHECRs above 60 EeV and the distribution of nearby AGN gives rise to the prediction that UHECRs may come from FR-I galaxies. Although FR-II galaxies would be a good candidate due to their high intrinsic luminosity, they are not abundant enough and too far away to lead to such a correlation. FR-I galaxies, on the other hand, have a much higher source density and there exist several nearby sources which could be responsible for a directional correlation. The most prominent FR-I galaxies are Cen A and M 87, as well as the flat spectrum radio sources BL Lac and Perseus A. Flat spectrum radio sources with low luminosities, called BL Lac objects, are typically interpreted as FR-I galaxies with their jet pointing directly towards Earth.

Observations of the jet structure of M 87 (Walker et al., 2008) and BL Lac (Marscher et al., 2008) near the central black hole indicate that, while there can be moving shocks between 10 and 1000 Schwarzschild-radii, the first strong, stationary shock occurs at $\sim$ 3000 Schwarzschild-radii (r_g), as already discussed by Markoff et al. (2001, 2005). This is further confirmed by Britzen et al. (2008) in the case of the BL Lac type object S5 1803+784. At $\sim 3000\, r_g$, the optical depth for proton interactions with photons from the disk is around 2%. With synchrotron photons from the jet as a target, the optical depth is $\sim$ 90% at the same distance from the central black hole. In both cases, the optical depth decreases with the distance from the black hole, $\tau_{p\gamma} \sim z_j^{-1}$. Therefore, we predict that neutrinos are produced in the narrow jet, close to the central black hole. Their emission is beamed due to the proton's highly relativistic motion along the jet. Therefore, neutrinos can only be observed for sources pointing directly towards Earth. Protons, on the other hand, dominantly arise in the last strong shock of the jet, at several kpc distance from the central black hole, where the optical depth is close to zero.

Using the correlation between UHECRs and the distribution of AGN as a measure for the Cosmic Ray flux from the supergalactic plane and connecting

this to the neutrino emission produced near the foot the AGN jet results in a predicted neutrino signal about an order of magnitude below the current AMANDA limit Achterberg et al. (2007). IceCube will be able to test this model within the first years of operation.

The general terms of this model are independent of Auger data, and could have been normalized to the established UHECR flux (Gaisser & Stanev, 2006), assuming that radio galaxies are the sources (Ginzburg & Syrovatskii, 1964; Biermann & Strittmatter, 1987, e.g.). Auger does confirm a correlation with the distribution of active galactic nuclei (Auger Collaboration, 2007, 2008), while HiRes (Abbasi et al., 2008a) does not, using the same energy threshold, and the same procedure. It is clear that more data are required, and the energy threshold might ultimately be seriously different; the results show that a confirmation from a larger data set will be necessary.

Acknowledgements

References

Abbasi, R. U., (HiRes Coll.), et al., 2008a. arXiv:0804.0382.
Abbasi, R. U., (HiRes Coll.), et al., 2008b. Phys. Rev. Let. 100 (10), 101101.
Abraham, J., (Auger Coll.), et al., 2008. Phys. Rev. Let. 101 (6), 061101.
Achterberg, A., (IceCube Coll.), et al., 2007. Phys. Rev. D 76 (4), 042008.
Albert, J., (MAGIC Coll.), et al., 2007. Astroph. Journal Let. 666, L17.
Atoyan, A., Dermer, C. D., 2001. Phys. Rev. Let. 87 (22), 221102.
Atoyan, A. M., Dermer, C. D., 2003. Astroph. Journal 586, 79.
Auger Collaboration, 2007. Science 318, 938, see also www.sciencemag.org.
Auger Collaboration, 2008. Astropart. Phys. 29, 188.
Ave, M., et al., 2005. Astropart. Phys. 23, 19.
Baring, M. G., 2004. Nucl. Phys. B Proc. Suppl. 136, 198.
Becker, J. K., 2008. Physics Reports 458, 173.

Becker, J. K., Biermann, P. L., Rhode, W., 2005. Astropart. Phys. 23, 355.

Becker, J. K., et al., 2006. In: TeV Particle Astrophysics II. http://www.icecube.wisc.edu/tev/proceedingfiles.php.

Bednarek, W., Protheroe, R. J., 1999. Mon. Not. of the Royal Astron. Soc. 302, 373.

Bednarz, J., Ostrowski, M., 1998. Phys. Rev. Let. 80, 3911.

Berezinsky, V., Gazizov, A., Grigorieva, S., 2006. Phys. Rev. D 74 (4), 043005.

Biermann, L., 1951. Zeitschrift für Astrophysik 29, 274.

Biermann, P. L., 1993. Astron. & Astroph. 271, 649.

Biermann, P. L., Strittmatter, P. A., 1987. Astroph. Journal 322, 643.

Blandford, R. D., 1976. Mon. Not. of the Royal Astron. Soc. 176, 465.

Blandford, R. D., Königl, A., 1979. Astroph. Journal 232, 34.

Blandford, R. D., Znajek, R. L., 1977. Mon. Not. of the Royal Astron. Soc. 179, 433.

Bouwens, R. J., Illingworth, G. D., 2006. Nature 443, 189.

Bridle, A. H., Perley, R. A., 1984. Ann. Rev. Astron. Astrophys. 22, 319.

Britzen, S., Kudryavtseva, N. A., Witzel, A., Campbell, R. M., et al., 2008. The kinematics in the pc-scale jets of AGN - The case of S5 1803+784. accepted for publication in A&A.

Caramete, L., et al., 2008. in preparation.

Cavaliere, A., Menci, N., 1997. Astroph. Journal 480, 132.

Cuoco, A., Hannestad, S., 2008. Phys. Rev. D 78 (2), 023007.

Curuţiu, A., et al., 2008. in preparation.

Das, S., et al., 2008. Astroph. Journal 682, 29.

Donea, A.-C., Biermann, P. L., 1996. Astron. & Astroph. 316, 43.

Duţan, I., Biermann, P. L., 2005. In: Shapiro, M. M., Stanev, T., Wefel, J. P. (Eds.), Neutrinos and Explosive Events in the Universe. p. 175.

Duţan, I., Biermann, P. L., 2008. In: Relativistic Astrophysics Legacy and Cosmology - Einstein's, ESO Astrophysics Symposia. Springer-Verlag Berlin Heidelberg.

Duţan, I., et al., 2008. in preparation.

Dunlop, J. S., Peacock, J. A., 1990. Mon. Not. of the Royal Astron. Soc. 247, 19.

Falcke, H., Biermann, P. L., 1995. Astron. & Astroph. 293, 665.

Falcke, H., Gopal-Krishna, Biermann, P. L., 1995a. Astron. & Astroph. 298, 395.

Falcke, H., Malkan, M. A., Biermann, P. L., 1995b. Astron. & Astroph. 298, 375.

Fanaroff, B. L., Riley, J. M., 1974. Mon. Not. of the Royal Astron. Soc. 167, 31P.

Fermi, E., 1949. Phys. Rev. 75 (8), 1169.

Fermi, E., 1954. Astroph. Journal 119, 1.

Gaisser, T. K., Halzen, F., Stanev, T., 1995. Phys. Rev. 258, 173.

Gaisser, T. K., Stanev, T., 2006. Nucl. Phys. A 777, 98.

Gallant, Y. A., Achterberg, A., 1999. Mon. Not. of the Royal Astron. Soc. 305,

L6.

Ginzburg, V. L., Syrovatskii, S. I., 1964. The Origin of Cosmic Rays. New York: Macmillan.

Gizani, N. A. B., Leahy, J. P., 2003. Mon. Not. of the Royal Astron. Soc. 342, 399.

Gopal-Krishna, Biermann, P. L., Wiita, P. J., 2004. Astroph. Journal Let. 603, L9.

Gopal-Krishna, et al., 2007. Mon. Not. of the Royal Astron. Soc. 377, 446.

Halzen, F., Hooper, D., 2002. Reports of Progress in Physics 65, 1025.

Halzen, F., O'Murchadha, A., 2008. arXiv:0802.0887.

Hillas, A. M., 1984. Ann. Rev. Astron. Astrophys. 22, 425.

Hoffmann, F. d., Teller, E., 1950. Phys. Rev. 80 (4), 692.

Hooper, D., Taylor, A., Sarkar, S., 2005. Astropart. Phys. 23, 11.

Iye, M., et al., 2006. Nature 443, 186.

Jokipii, J. R., 1987. Astroph. Journal 313, 842.

Kachelriess, M., Ostapchenko, S., Tomas, R., 2008. arXiv:0805.2608.

Kardashev, N. S., 1962. Astronomicheskii Zhurnal 39, 393, english translation in Soviet Astron. AJ, **6**:317 (1962).

Koers, H. B. J., Tinyakov, P., 2008. arXiv:0802.2403.

Komatsu, E., et al., 2008. ArXiv: 0803.0547 Submitted to ApJ Supp. Series.

Krülls, W. M., 1992. Astron. & Astroph. 260, 49.

Lind, K. R., Blandford, R. D., 1985. Astroph. Journal 295, 358.

Lovelace, R. V. E., 1976. Nature 262, 649.

Mach, E., 1898. Über Erscheinungen an fliegenden Projektilen. Separatum ex. Ver. nw. Kenntn., Wien.

Mach, E., Wentzel, J., 1884. Anzeiger der Kaiserliche Akademie der wissensch., Math. Naturw. Classe, Wien, experimental setup.

Mach, E., Wentzel, J., 1885. Kaiserliche Akademie der wissensch., Math. Naturw. Classe, Wien, experimental results.

Malkan, M. A., Sargent, W. L. W., 1982. Astroph. Journal 254, 22.

Mannheim, K., 1995. Astropart. Phys. 3, 295.

Mannheim, K., Protheroe, R. J., Rachen, J. P., 2001. Phys. Rev. D 63, 23003.

Mannheim, K., Stanev, T., Biermann, P. L., 1992. Astron. & Astroph. 260, L1.

Markoff, S., Falcke, H., Fender, R., 2001. Astron. & Astroph. 372, L25.

Markoff, S., Nowak, M. A., Wilms, J., 2005. Astroph. Journal 635, 1203.

Marscher, A. P., et al., 2008. Nature 452, 966.

Massi, M., Kaufman Bernadó, M., 2008. Astron. & Astroph. 477, 1.

Meisenheimer, K., et al., 1989. Astron. & Astroph. 219, 63.

Meli, A., Becker, J. K., Quenby, J. J., 2007. In: 30th International Cosmic Ray Conference. arXiv:0708.1438.

Meli, A., Becker, J. K., Quenby, J. J., 2008. A&A, in press. (arXiv:0709.3031).

Meli, A., Biermann, P. L., 2006. Astron. & Astroph. 454, 687.

Miley, G., 1980. Ann. Rev. Astron. Astrophys. 18, 165.

Münich, K., et al., 2007. In: 30th International Cosmic Ray Conference. astro-

ph/0711.0353.

Narayan, R., Yi, I., 1995. Astroph. Journal 452, 710.

Nellen, L., Mannheim, K., Biermann, P. L., 1993. Phys. Rev. D 47, 5270.

Novikov, I. D., Thorne, K. S., 1973. Astrophysics of black holes. In: DeWitt, C., DeWitt, B. (Eds.), Black Holes (Les Astres Occlus). Gordon & Breach, NY, p. 343.

Nulsen, P. E. J., et al., 2005. Astroph. Journal Let. 625, L9.

O'Dea, C. P., Baum, S. A., 1997. Astron. Journ. 113, 148.

Parker, E. N., 1958. Astroph. Journal 128, 664.

Roth, M., 2008. priv. comm.

Rybicki, G. B., Lightman, A. P., 1979. Radiative processes in astrophysics. J. Wiley & Sons, Inc.

Ryu, D., et al., 2008. Science 320, 909.

Sanders, R. H., 1983. Astroph. Journal 266, 73.

Shakura, N. I., Sunyaev, R. A., 1973. Astron. & Astroph. 24, 337.

Stanev, T., 2004. High Energy Cosmic Rays. Springer-Verlag.

Stecker, F. W., 2005. Phys. Rev. D 72 (10), 107301.

Stecker, F. W., Baring, M. G., Summerlin, E. J., 2007. Astroph. Journal Let. 667, L29.

Taşcău, O., 2003. Master's thesis, Univ. of Bukarest.

Urry, C. M., Padovani, P., 1994. In: Bicknell, G. V., Dopita, M. A., Quinn, P. J. (Eds.), The Physics of Active Galaxies. Vol. 54 of Publ. of the Astron. Soc. of the Pac. p. 215.

Urry, C. M., Padovani, P., 1995. Publ. of the Astron. Soc. of the Pac. 107, 803.

Véron-Cetty, M.-P., Véron, P., 2006. Astron. & Astroph. 455, 773.

Völk, H. J., Biermann, P. L., 1988. Astroph. Journal Let. 333, L65.

Walker, R. C., et al., 2008. arXiv:0803.1837.

Whysong, D., Antonucci, R., 2003. New Astron. Rev. 47, 219.

Willott, C. J., et al., 2001. Mon. Not. of the Royal Astron. Soc. 322, 536.

Zier, C., Biermann, P. L., 2002. Astron. & Astroph. 396, 91.